Numerical Study of Effects of Inhomogeneous Roughness on the Ship Friction Resistance

Rajabal Akbar[1], *I Ketut* Suastika[1]*, and *I Ketut Aria Pria* Utama[1]

[1]Department of Naval Architecture, Sepuluh Nopember Institute of Technology (ITS), 60111 Surabaya, Indonesia

Abstract. The cleanliness of a ship hull is crucial for energy saving. Biofouling, which can cause microbiological corrosion, can also increase ship resistance. If left unchecked, this can lead to inefficient energy use and increased emissions, contributing to global warming. Ship resistance is a critical factor in ship design, which affects ship powering. The analysis of friction resistance due to biofouling on a ship hull requires an examination of the distribution of roughness height (k_s), which is randomly distributed. In this study, an analysis of friction resistance coefficient (C_F) due to inhomogeneous roughness is carried out with the help of CFD simulations with a full-scale model at 19 kn and 24 kn. The roughness of three ship segments, namely aft-hull, midship, and fore-hull, varies with ks values of 125 μm (P), 269 μm (Q), and 425 μm (R), respectively, while maintaining the same wetted surface area (S) in each segment. According to the simulation results, the RQP model produces the highest C_F of 2.154 x 10^{-3}, while the PQR model produces the smallest C_F of 2.119 x 10^{-3} each at speed 24 knots. The C_F contributes an average of 72.2% C_T.

1 Introduction

Frictional resistance is typically 60%–70% of total hull resistance for tankers, bulk carriers and container ships, and any reduction in this component can have significant benefits [1]. Hull surface finish is fundamental to the levels of hull skin friction resistance. A smooth surface, with low roughness, will normally lead to lower frictional and viscous pressure resistance. However, in actual conditions, ships that have been in operation for a certain period become overgrown with biofouling, resulting in decreased ship performance.

Preventing biofouling on ship hulls is crucial to avoid energy waste and reduce emissions that contribute to global warming. Biofouling can cause the hull surface to become rough, increasing friction resistance, This has been proven by Schultz [2], Turan et al. [3], Song et al. [4], and numerous others.

In addition to increasing friction resistance, the roughness of a ship hull can also affect its residual resistance. Demirel et al. [5] and Song et al. [6] studied this phenomenon using the CFD simulation method on the KCS ship hull model. The results showed that as the hull becomes rougher, the ΔC_F value increases while the ΔC_W value decreases. According to the ITTC procedure [7], roughness affects only the C_F value. Therefore, the procedure includes

*Corresponding author: k_suastika@na.its.ac.id

a formula to calculate the *ΔCF* value. This formula is based on the *ΔCF* formula developed by Bowden and Davidson [8] and Hakim et al. [9].

An alternative to experimental and empirical methods is the numerical method using computational fluid dynamics (CFD). In addition, given that the hull's three-dimensional geometry has been considered in CFD, and the ship can be simulated at full-scale, ship resistance estimates are more accurate [6]. As a result, several recent research have employed the CFD approach to investigate the effect of roughness on ship resistance. [5] and [10]. Suastika et al., [11] conduct a simulation using a resolved Reynolds-averaged Navier-Stokes (RANS) Computational Fluid Dynamics (CFD) simulation to determine the resistance of a newly cleaned and painted hull (orange peel roughness) [12]. There have been many attempts to characterize and simulate the increase in skin tinkering drag due to ship hull roughness in the last three decades, including by performing CFD simulations.

This study investigates the effect of inhomogeneous roughness on the endurance of KCS vessels at speeds of 19 and 24 knots. The research highlights the significance of maintaining a clean ship hull to conserve energy and decrease emissions. It also investigates the impact of microbiological corrosion caused by biofouling, which can reduce ship durability and impede energy efficiency. This study analyzes the friction resistance coefficient (C_F) resulting from inhomogeneous roughness (125 μm, 269 μm, and 425 μm) distributed over three vessel segments (aft-hull, midship, and fore-hull) with differences in roughness height for each segment using Computational Fluid Dynamics (CFD) simulations with full-scale modeling. The aim is to approach actual conditions where the height of roughness on the surface of the ship's hull is distributed randomly and unevenly. This investigation uses the Reynolds-Averaged Navier-Stokes (RANS) equations to reveal a correlation between increased roughness and higher friction resistance. The findings provide valuable insights for ship design and maintenance practices. The methodology combines the k-ω SST turbulence model and Reynolds decomposition for accurate numerical modeling, which is validated through comparison with existing data. The research findings have significant implications for ship design, maintenance, and environmental considerations. They contribute to optimizing ship performance and reducing energy consumption. Therefore, it is essential to address biofouling and maintain ship hull cleanliness for sustainable maritime operations.

2 Methodology

2.1 Ship Friction Resistance

The total resistance of a KCS hull (R_T) is primarily composed of two components: the residuary resistance (R_R) and the frictional resistance (R_F), as given by Eq. (1).

$$R_T = R_F + R_R \tag{1}$$

After obtaining the total drag values (R_T) for each related speed, the non-dimensional form of R_T was calculated by dividing each term by the dynamic pressure (the product of half the water density ρ and the velocity squared v^2) and wetted surface area (S). This resulted in the total drag coefficient (C_T) which was calculated using the following Eq. (2).

$$C_T = \frac{R_T}{\frac{1}{2}\rho\, S\, v^2} \tag{2}$$

Friction resistance is a component of resistance related to the force generated by friction between fluid molecules and against surfaces. It depends on the wet surface area of the ship's hull, the level of roughness, and the Reynolds number, generally shown by Eq. (3)

$$C_F = \frac{R_F}{\frac{1}{2}\rho\, S\, v^2} \tag{3}$$

The simulation results provide direct values for total resistance (R_T) and frictional resistance (R_F), which can be calculated in non-dimensional form as coefficients (C_T) and (C_F).

2.2 Numerical Formulations

In general, fluid flow in technology applications is turbulent. Turbulence occurs when the inertial force dominates over the viscous force, which dampens instability in the flow. The Reynolds number, which is the ratio of the inertial force to the viscous force, determines the onset of turbulence [13]. The solution to turbulent flow is, in principle, the solution to the conservation laws that govern fluid flow, specifically the Navier-Stokes equation. To identify the turbulent flow solution, a turbulence modeling approach can be taken, such as the Reynolds-Averaged Navier-Stokes (RANS) equation. This equation is obtained by averaging the Navier-Stokes equation using the Reynolds decomposition method. The RANS equation for incompressible flow comprises the continuity, and impulse [14],

Continuity equation:

$$\nabla.[\rho U] = 0 \tag{4}$$

Momentum equation:

$$\frac{\partial[\rho U]}{\partial t} + \nabla.\{\rho UU\} = -\nabla P + \left[\nabla.\left\{\bar{\tau}_{ij} - \rho\overline{u'u'}\right\}\right] + \rho g \tag{5}$$

The k-ω SST model [12] is used to calculate the Reynolds stress $-\rho\overline{u'u'}$ to solve the system of Eqs. (4) and (5).

2.3 Geometry and Boundary Conditions

Figure 1 shows a schematic illustration of roughness arrangements of the CFD methodology. Roughness modeling on full scale KCS ships was carried out by creating a roughness arrangement design (PQR, PRQ, QPR, QRP, RPQ, RQP) with three roughness variations, namely low roughness P = 125 μm, medium roughness Q = 269 μm and high roughness R = 425 μm). The three variations in roughness values are arranged into three ship segments (fore-hull, midship, and aft-hull), which are divided to have the same wetted surface area (*S*). The six roughness arrangements are shown in detail in Table 1 and Figure 1,

Table 1. The variation of roughness values

Roughness arrangement	k_s (μm) Fore hull	k_s (μm) Midship	k_s (μm) Aft hull
PQR	125	269	425
PRQ	125	425	269
QPR	269	125	425
QRP	269	425	125
RPQ	425	125	269
RQP	425	269	125

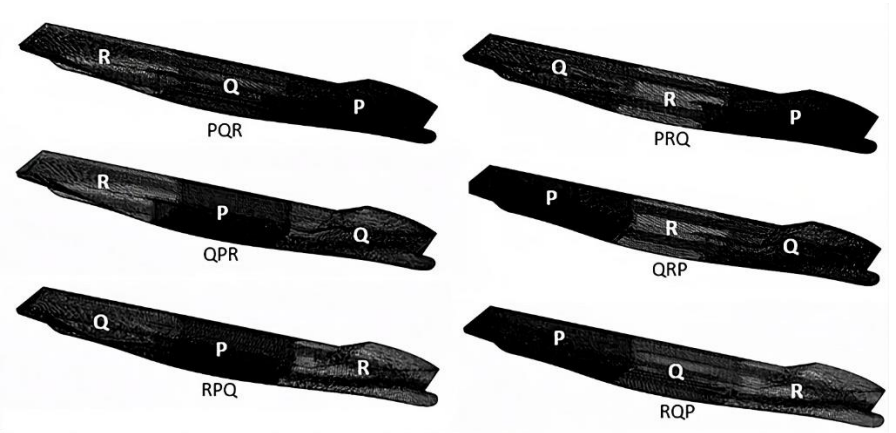

Fig. 1. Roughness arrangements for three ship segments (fore-hull, midship, and aft-hull)

Figure 2 shows the boundary conditions settings on the half body,

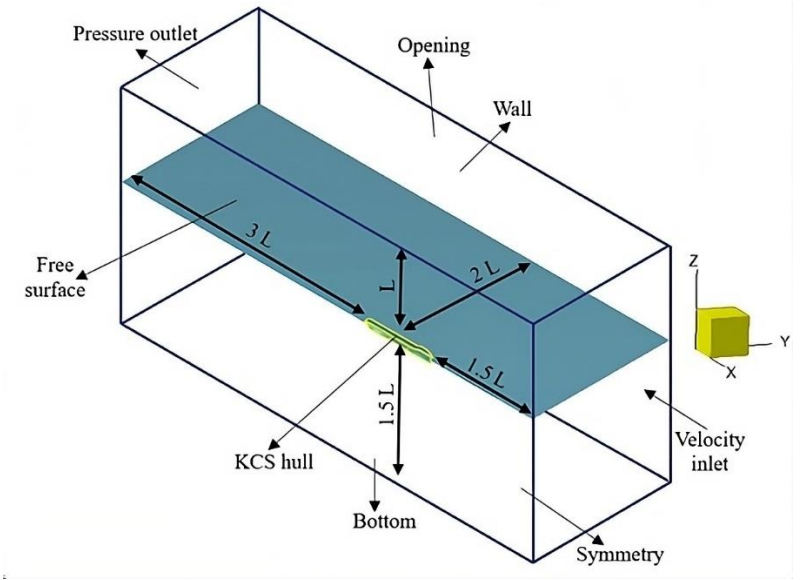

Fig. 2. Boundary conditions dimension (half body)

Figure 2 specifies the domain dimensions and boundary conditions. Only half of the hull body is included to model the symmetrical flow field. The following boundary conditions are applied: a wall function is imposed on the hull surface, the far field velocity condition is applied to the opening, wall, and bottom, a symmetry condition is used for the hull center plane, the flow velocity at the inlet is defined as the tested speed, and at the outlet, the hydrostatic pressure defined as a function of water level height is applied.

2.4 Mesh generation

Meshings are created using NUMECA HEXPRESS software, which has features for creating meshings and domain manipulation functions for the simulation domain. The meshing manufacturing process consists of initial mesh, adaptation to geometry, snap to geometry, optimization, and viscous layers. The detailed grid generation is shown in Figure 3.

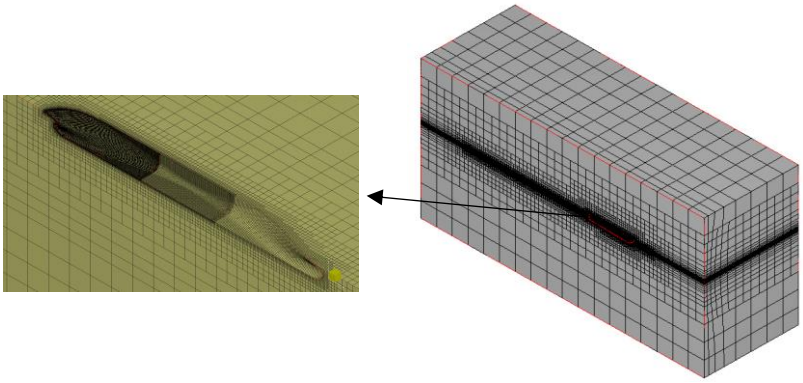

Fig. 3. Grid generation

Figure 3 shows an all-hexahedral unstructured grid generation system during the meshing process. The purpose of grid generation in CFD is to define a numerical mesh throughout the system to be simulated. This process is crucial because the grid selected for CFD simulations defines the accuracy and resolution of the simulation results, both of which affect the computation time and level of detail in the results.

Section 3 contains report figures that will aid in understanding the impact of increased hull roughness on ship resistance for various hull conditions.

3 Results and Discussion

3.1 Effects of Inhomogeneous Roughness on Ship Resistance

The CFD simulation has been carried out in full viscous conditions, where from the results of running the CFD, direct frictional resistance (R_F). The resistance data is multiplied by two because the CFD running is only done on half of the hull. This is done to minimize simulation time to make the simulation more effective. Figure 4 shows the C_F value for each roughness arrangement,

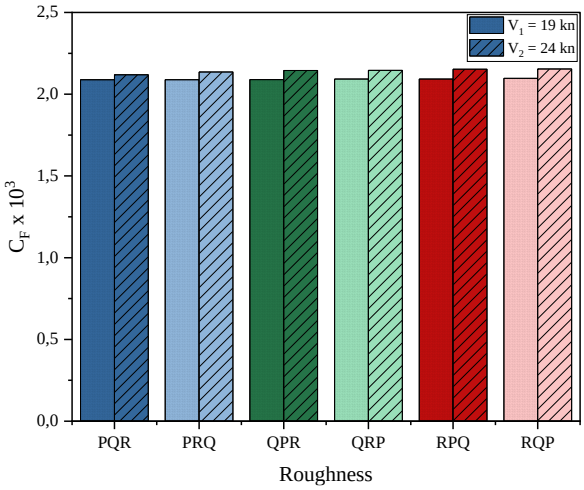

Fig. 4. Friction resistance coefficient C_F for each roughness arrangement.

Figure 4 shows a significant increase in the C_F value. The C_F sequence, from lowest to highest, is PQR < PRQ < QPR < QRP < RPQ < RQP. The PQR configuration produces the lowest C_F 2.119 x 10^{-3}, while the RPQ model has the highest C_F 2.154 x 10^{-3}. The increase in turbulence and decrease in speed profile caused by the transition from a surface with low roughness to one with higher roughness results in an increase in frictional resistance. In detail, the C_F composition of each configuration can be seen in Figure 5.

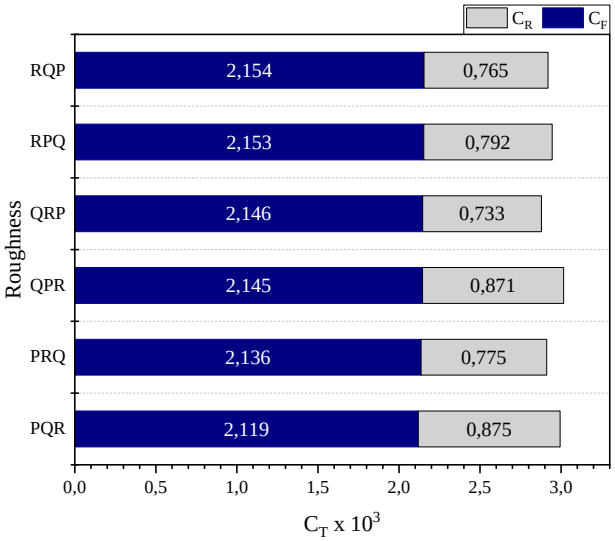

Fig. 5. Total resistance coefficient (C_T) of the KCS hull for speed V = 24 knots and inhomogeneous roughness surfaces

Figure 5 illustrates that the C_F dominates the total resistance by 72.5% of C_T in each condition, and in general, it can be seen that the reduction in C_F is proportional to the increase in C_R. The frictional resistance of fluids interacting with passing objects is affected by their viscosity. Therefore, the geometry of a ship's hull shape, which is influenced by differences in roughness in each segment through which the fluid passes, will affect the local frictional resistance value. This, in turn, impacts the overall C_F value.

The validation of the CFD results for modeling roughness effects on ship resistance is crucial to ensure accurate and reliable simulation results. To achieve this, compared the inhomogeneous roughness hull with a smooth hull surface without roughness and a homogeneous roughness hull. As shown by the bar diagram in Figure 6, by adopting the conference paper data by Akbar et al. [15] for KCS without roughness and KCS with homogeneous roughness, which has been validated with the ITTC 1957 equation and data of Demirel et al [5].

The bar chart in Figure 6 shows that at V_1 speed, C_F PPP model increases by 1.6% compared to smooth model (SSS). As the roughness height increases, C_F continues to increase up to 57.1% at RRR model. At a V_1 speed, the average C_F value in the inhomogeneous roughness model falls between the range of homogeneous C_F values PPP and QQQ at 2.09 x 10^{-3}. The same occurs at a V_2 speed, with the average C_F value at 2.14 x 10^{-3}, where the C_F value for each model with inhomogeneous roughness falls between the C_F PPP and C_F QQQ ranges. The change in flow velocity at each k_s transition causes this phenomenon.

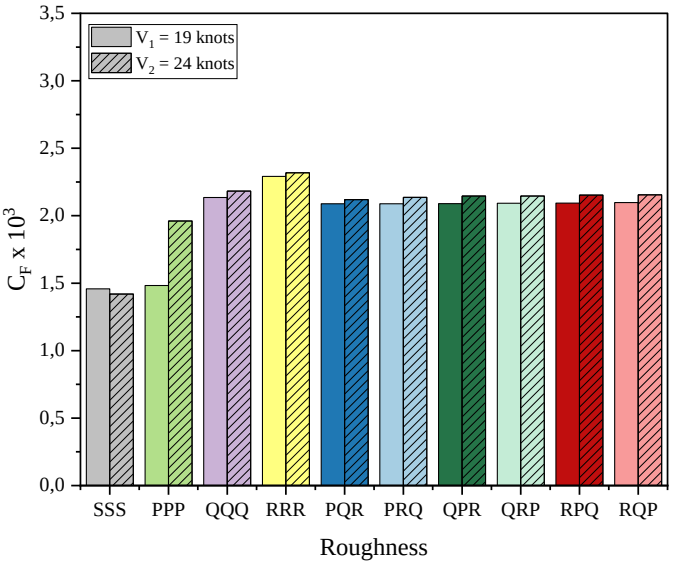

Fig. 6. Comparison of C_F values in conditions without roughness, with homogeneous roughness, and with inhomogeneous roughness.

When the fore-hull section has minimum roughness (PQR and PRQ), the resulting C_F is smaller than the fore-hull with greater roughness (RPQ and RQP). This phenomenon occurs because the flow transition on a surface with a high level of roughness to a lower level of roughness causes a decrease in turbulence and an increase in the speed profile in that area, resulting in a reduction of friction resistance. Figure 6 shows that as speed increases, the C_F of KCS without roughness decreases, while for KCS with roughness, the C_F value increases. This is due to the transition from a surface with low roughness to one with higher roughness, which increases turbulence and decreases the speed profile, increasing frictional resistance. Conversely, for KCS ships without roughness, frictional resistance decreases at high speeds. At high speeds, the wave-making resistance becomes more significant while the frictional resistance becomes less dominant. Therefore, the decrease in frictional resistance for KCS ships without roughness at high speeds is due to increased wave-making resistance. This results in line with Song et al. [16], it is observed that the C_F values for the rough KCS model remain relatively constant with the Reynolds numbers, while the smooth C_F values exhibit a

decreasing trend. This behavior can be explained by the fact that the C_F becomes less dependent on the Reynolds number as it approaches the fully rough regime, as indicated by Nikuradse's work in 1933 [17], and supported by studies Demirel et al. [5], and Song et al. [6].

3.2 Visualization of Wall Shear Stress on the KCS Hull

Increased surface roughness can lead to viscous stress conditions, illustrated in Figure 7. The figure shows the differences in viscous stress created in the transition section of the roughness level of the KCS hull based on the CFD simulation results. The relationship between roughness and viscous stress is proportional to the ship's frictional resistance increase. The same effect occurs when the speed is increased. According to the RQP model, the flow or velocity profile moves from the fore-hull (roughness R) to the midship (roughness Q) and exits at the aft-hull (roughness P), and so on for the other five models. The model with the highest roughness (R) is placed in the stern segment (aft-hull) in the QPR and PQR models, giving a relatively higher C_F than other models. The model with the lowest roughness (P) at the stern (aft-hull) provides an advantage over the C_F quantity with the minimum value among the other models, namely the RQP and QRP models. This occurs because a high level of roughness on the surface of the ship's stern causes an increase in turbulence and a decrease in the speed profile in that area, increasing frictional resistance.

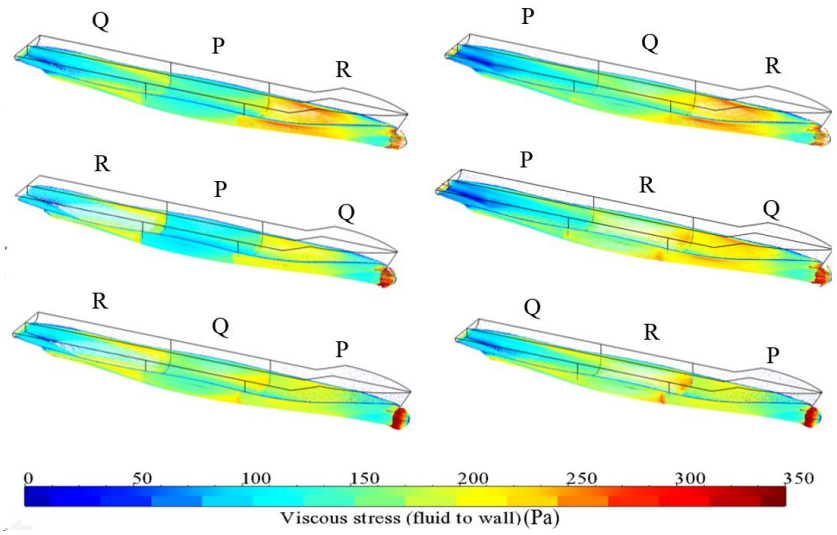

Fig. 7. The high and low shear stress values in the roughness change transition area.

3.3 Wave Pattern Visualization on the Free Surface Area of the KCS Hull

The visualization and analysis of wave patterns contribute to a comprehensive understanding of the hydrodynamic behavior of the KCS hull, particularly wave pattern and total resistance and the influence of different roughness conditions, as seen in Figure 8. The effect of the wave phenomenon in Figure 8 indicated the resulting friction resistance, where for the smallest friction resistance, namely at PQR, the wave pattern on the aft-hull section is green to yellow, is not as dominant as in the RQP model, where the wave elevation with maximum height is more dominant on the aft-hull.

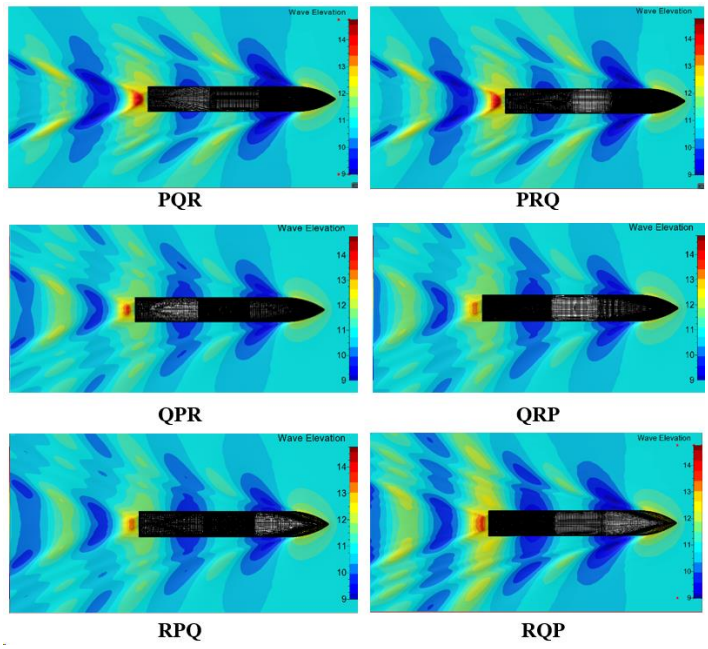

Fig. 8. Wave pattern of the KCS for inhomogeneous roughness at $V_2 = 24$ kn

Figure 8 RQP shows a high wave elevation in the aft area of the hull (dominated in yellow), indicating that wave resistance dominates the drag, and friction resistance is relatively small compared to PQR where the wave elevation is small (aft-hull less yellow). Correlating wave patterns with flow velocity profiles is critical, providing insight into how wave patterns and associated resistance change with varying velocity profiles. As the flow velocity profile increases (transition from low to high roughness P to Q, Q to R, and P to R), the waves generated by the ship increase due to increased turbulence, and the resistance is almost entirely influenced by the elevation of the waves formed so that the total resistance is dominated by the resistance wave or residual. On the other hand, when the velocity profile decreases due to the flow transition from a surface from high to low roughness (Q to P, R to Q, and R to P), the resulting wave energy decreases. At that time, the fluid is viscous, so the total resistance is predominantly influenced by viscous resistance, and if divided by the shape factor (1+k), it will produce friction resistance.

4 Conclusions

This research uses the Reynolds-averaged Navier-Stokes (RANS) equations and the k-ω SST turbulence model to predict frictional resistance. This research applies the roughness function to assess the impact of surface roughness on resistance by simulating flow under varying surface roughness conditions. The findings show that increasing surface roughness results in higher drag forces, especially in models with fore-hulls that have high roughness, with the order of friction coefficient (C_F) from low to high, namely PQR < PRQ < QPR < QRP < RPQ < RQP. Studies show that the transition from low to high surface roughness increases turbulence and reduces velocity, resulting in higher friction resistance. This can be visualized through the CFD results' shear stress contours and wave patterns. This information is critical for specifying a ship's propulsion system, estimating fuel consumption, and evaluating the impact of biofouling on overall ship performance. This research approach and findings

contribute to a better understanding of the impact of surface roughness on ship resistance, with potential implications for ship design and maintenance.

Acknowledgement

The authors greatfully acknowledge the DIKTI scholarship from Ministry of Education and Culture namely BPPDN 2019 for funding this research.

References

1. R. Ravenna, S. Song, W. Shi, T. Sant, C. D. M. M. Fenech, T. Tezdogan, Y. K. Demirel. "CFD analysis of the effect of heterogeneous hull roughness on ship resistance," *Ocean Eng.*, vol. **258**, p. 111733, (2022), doi: 10.1016/j.oceaneng.2022.111733.
2. M. P. Schultz, "Effects of coating roughness and biofouling on ship resistance and powering," *Biofouling*, vol. **23**, no. 5, pp. 331–341, (2007), doi: 10.1080/08927010701461974.
3. O. Turan, Y. K. Demirel, S. Day, and T. Tezdogan, "Experimental Determination of Added Hydrodynamic Resistance Caused by Marine Biofouling on Ships," in *Transportation Research Procedia*, (2016), vol. **14**, pp. 1649–1658. doi: 10.1016/j.trpro.2016.05.130.
4. S. Song, R. Ravenna, S. Dai, C. D. M. M. Fenech, G. Tani, Y. K. Demirel, M. Atlar, S. Day, A. Incecik. "Experimental investigation on the effect of heterogeneous hull roughness on ship resistance," *Ocean Eng.*, vol. **223**, p. 108590, (2021), doi: 10.1016/j.oceaneng.2021.108590.
5. Y. K. Demirel, O. Turan, and A. Incecik, "Predicting the effect of biofouling on ship resistance using CFD," *Appl. Ocean Res.*, vol. **62**, pp. 100–118, (2017), doi: 10.1016/j.apor.2016.12.003.
6. S. Song, Y. K. Demirel, and M. Atlar, "An investigation into the effect of biofouling on the ship hydrodynamic characteristics using CFD," *Ocean Eng.*, vol. **175**, pp. 122–137, (2019), doi: 10.1016/j.oceaneng.2019.01.056.
7. "ITTC-Recommended Procedures and Guidelines CFD, General CFD User's Guide."7.5-03.01-03. (1999).
8. B. Bowden and N. Davidson, "Resistance Increment Due to Hull Roughness Associated with Form Factor Extrapolation Methods," in *National Physical Laboratory (NPL) Ship technical Manual 3800*, (1974).
9. M. L. Hakim, I. K. Suastika, and I. K. A. P. Utama, "A practical empirical formula for the calculation of ship added friction-resistance due to (bio)fouling." *Ocean Eng*, **271**, 113744 (2023), https://doi.org/10.1016/j.oceaneng.2023.113744
10. M. L. Hakim, B. Nugroho, R. C. Chin, T. Putranto, I. K. Suastika, and I. K. A. P. Utama, "Drag penalty causing from the roughness of recently cleaned and painted ship hull using RANS CFD," *CFD Lett.*, vol. **12**, no. 3, pp. 78–88, (2020), doi: 10.37934/cfdl.12.3.7888.
11. I. K. Suastika, M. L. Hakim, B. Nugroho, A. Nasirudin, I. K. A. P. Utama, J. P. Monty, B. Ganapathisubramani., "Characteristics of drag due to streamwise inhomogeneous roughness," *Ocean Eng.*, vol. **223**, p. 108632, (2021), doi: 10.1016/j.oceaneng.2021.108632.
12. I. K. A. P. Utama, B. Nugroho, M. Yusuf, F. A. Prasetyo, M. L. Hakim, I. K. Suastika, J. P. Monty., "The Efect of Cleaning and Repainting on the Ship Drag Penalty,"

Biofouling, vol. **37**, no. 4, pp. 372–386, (2021).

13. I. K. Suastika, *Dinamika Fluida Komputasi- Metode Volume Hingga*, 1st ed. Surabaya: ITS Press, (2023).
14. M. Moukalled, F., Mangani, L., & Darwish, "The finite volume method," *Springer Int. Publ.*, pp. 103–135, (2016).
15. R. Akbar, I. K. Suastika, and I. K. A. P. Utama, "Numerical Study of Effects of Homogeneous Roughness on the Friction Resistance," in *SENTA*, p. ID-132, (2023).
16. S. Song, K. Demirel, M. Atlar, S. Dai, S. Day, and O. Turan, "Validation of the CFD approach for modelling roughness effect on ship resistance." *Ocean Eng.*, vol. **200**, p. 107029, (2020). https://doi.org/10.1016/j.oceaneng.2020.107029.
17. J. Nikuradse, "Gesetzmäßigkeiten der turbulenten Strömung in glatten Rohren (Nachtrag)," *Forsch. auf dem Gebiet des Ingenieurwesens A*, vol. **4**, no. 1, p. 44, (1933).